Title: Foveolar drusen decrease fixation stability in pre-symptomatic AMD.

Authors: J. Murari[1], J. Gautier[2], J. Daout[1], L. Krafft[3], P. Senée[3,4], P. Mecê[3,5], K.Grieve[1,2], W. Seiple[6], S. Meimon[3], *D. Sheynikhovich[1], M. Paques[2], A. Arleo[1]

Financial support: IHU FOReSIGHT (ANR-18-IAHU-01), SilverSight (ANR-18-CHIN-0002), OPTORETINA ERC (101001841), UNADEV / Aviesan 2020.

Conflict of interest: No conflicting relationship relevant for this manuscript exists for any author.

Running title: Foveolar drusen decrease fixation stability

This article contains two video clips as additional online-only material. They should appear online as: *Clip 1* and *Clip 2*.

This article contains additional online-only figures. They should appear online as: *Supplemental Figure 1* and *Supplemental Figure 2*.

Abbreviations:

FEM: fixational eye movements

AMD: age-related macular degeneration

RPE: retinal pigment epithelium

AO-FIO: adaptive optics flood illumination ophthalmoscope

RMS-S2S: root mean square sample-to-sample

ISOA: isoline area

SD-OCT: spectral domain optical coherence tomography

Key words: AMD, drusen, fixational eye movements, fovea

[1]Sorbonne Université, INSERM, CNRS, Institut de la Vision, France ; [2]CHNO des Quinze-Vingts, INSERM-DGOS CIC, France ; [3]Office National d'Etudes et de Recherches Aérospatiales (ONERA), France ; [4]Quantel Medical SA, France ; [5]Institut Langevin, CNRS, ESPCI France ; [6]Lighthouse Guild, United States

J. Murari and J. Gautier contributed equally to this work

*Corresponding author: Denis Sheynikhovich (denis.sheynikhovich@sorbonne-universite.fr)

Abstract

Purpose: To link changes of fixational eye movements (FEM) in controls and patients with foveal drusen using adaptive optics retinal imaging to find anatomo-functional markers for pre-symptomatic Age-related Macular Degeneration (AMD).

Design: A population-based cohort study.

Participants: 7 young controls, 4 older controls and 16 presymptomatic AMD patients with foveal drusen.

Methods: A high speed research-grade adaptive optics flood illumination ophthalmoscope was used for monocular retinal tracking of fixational eye movements. The system allows for sub-arcminute resolution, high-speed and distortion-free imaging of the foveal area. Early signs of AMD were documented using gaze-dependent imaging on a clinical-grade AO-FIO.

Main outcome measures: Microsaccade amplitude, drift diffusion coefficient and fixation stability across participants, and in the case of presymptomatic AMD participants, the relationship between these variables and retinal structure characteristics such as drusen size and eccentricity.

Results: FEM were measured with high precision (RMS-S2S=0.0015° on human eyes) and small foveal drusen (median=60μm) were detected with high contrast imaging. Microsaccade amplitude, drift diffusion coefficient and ISOline Area (ISOA) were significantly larger for patients with foveal drusen compared with controls. Among the drusen participants, microsaccade amplitude was correlated to drusen eccentricity from the center of the fovea.

Conclusions: A novel high-speed high-precision retinal tracking technique allowed for the characterization of FEM at the microscopic level. Foveal drusen altered fixation stability, resulting in compensatory FEM changes. Eye movement analysis with flood imaging provides robust description of both functional and structural signs of early age-related changes.

Introduction

Age-related macular degeneration (AMD) is the main cause of vision loss in developed countries, affecting 180M people in 2020 with an expected prevalence of 288M by 2040[1]. AMD starts with the accumulation of extracellular deposits, called drusen, in-between the Bruch's membrane and the retinal pigment epithelium (RPE). Multiplication and expansion of drusen is associated with late stages of AMD, which are classified into exudative (wet-AMD) and/or atrophic (dry-AMD)[2]. Wet-AMD is caused by irregular blood vessel growth (i.e., neovascularization) at the macular level, and it affects approximately 10-20% of AMD patients[3]. Although macular neovascularization can be successfully treated using anti-VEGF therapies, these treatments do not prevent the development of atrophy, which causes sight loss in the long term[4]. Geographic atrophy or dry-AMD is the irreversible loss of photoreceptors caused either by drusen development or neovascular growth, and it accounts for about 80 to 90% of the cases[2]. No effective treatment currently exists for this form of AMD. The absence of efficient treatment strategies for the late-stage AMD is exacerbated by the fact that patients frequently remain unaware of their AMD condition[5], so that they typically receive a diagnosis only upon the emergence of clinical indications, often at a stage too advanced for effective implementation of preventive strategies. There is therefore an urgent need to characterize anatomo-functional relationships associated with the earliest asymptomatic AMD stages aiming at complementing existing medical imaging techniques with functional measures of retinal anomalies that can serve as biomarkers of future disease onset. If indeed the pre-symptomatic structural anomalies are associated with functional, e.g. oculomotor, changes, their timely detection may also incite the individuals with a risk of developing AMD to engage in risk mitigation strategies to delay AMD onset and progression[6,7,8].

The objective of the present study is to test the novel hypothesis that the appearance of drusen, an early structural anomaly in presymptomatic AMD, is associated with detectable changes in microscopic eye movements during ocular fixation. Even though the development of early-to-late stages of confirmed AMD has already been associated with changes in fixation stability, decreased visual acuity, reduced visual field, slower reading speed, lower contrast sensitivity, and an overall deterioration of functional vision useful for daily activities[9–11], these previous studies did not explore fixational eye movements in presymptomatic stages, nor did they characterize the link between retinal structure changes and fixational eye movements. In patients with central scotomas, fixation stability as assessed

by retinal motion compensation strategies has been shown to worsen with AMD progression[12]. Moreover, advanced geographic atrophies were reported to affect different components of fixational eye movements, such as microsaccades (small saccades of amplitude below 1°) and ocular drift[13,14] (random Brownian-walk-like eye movements between microsaccades). More specifically, these studies report higher microsaccade amplitudes associated with macular lesions[13] and lower spectral whitening of natural scenes by ocular drift in patients with long-lasting macular disease, compared to age-matched controls[14]. Given the significant changes in fixational stability in advanced forms of AMD, it is important to test whether even the first signs of potential future disease can induce changes in eye movement statistics.

The hypothesis was tested by simultaneously performing *(i)* high-resolution retina imaging to visualize and characterize small asymptomatic alterations of the foveal structure, *(ii)* high-speed retina tracking to detect fixational eye movements, and *(iii)* precise retina stimulation to perform fine psychometrics. We studied the relationship between subtle structural retinal anomalies and fixational eye movement characteristics by examining healthy controls and participants with foveal drusen, but no scotoma or atrophy according to conventional measures. If the appearance of first drusen indeed leads to fixation instability, as the current study shows, such a structure-function relationship provides the possibility to use fine oculomotor measurements to predict the appearance of retinal anomalies and therefore contribute to the development of early anatomo-functional biomarkers for urgently needed screening approaches in presymptomatic AMD.

Methods

Participants

A cohort of 39 participants were recruited for the study as part of one of three groups: young controls (n=7, [2 females], age=31±7 yo), older controls (n=20, [14 females], age=75±4 yo) and drusen participants (n=12, [8 females], age=79±3 yo). The initial assignment of participants to the groups relied on the detection of drusen by standard spectral-domain optical coherence tomography (SD-OCT) imaging (Spectralis OCT, Heidelberg Engineering, Germany). All participants were recruited from the

101 SilverSight cohort[15], and they were fully screened and ascertained not to suffer from any age-related
102 sensory, cognitive, or motor pathology.

103 Prior to the beginning of the experiment, older controls and drusen participants were screened
104 using a novel imaging method, developed previously in our laboratory using Adaptive Optics Flood
105 Illumination Ophthalmoscope (AO-FIO, rtx1, Imagine Eyes), which is capable of detecting foveal drusen
106 not visible in standard SD-OCT or fundus imaging[16] (see the next section). As a consequence, 9
107 participants that had initially been recruited as older controls were actually found to have drusen in the
108 foveal region, and they were thus moved into the drusen group. In addition, a total of 12 participants
109 had to be excluded from study: 3 because of too blurry retina images on the rtx1; 3 due to poor signal-
110 to-noise ratio during the fixation task; 2 because of they were not fixating the right target; 3 because of
111 excessive tiredness and discomfort during the experiment; and 1 because she exhibited fixation
112 patterns typical of another disease. As a result, a total of 27 participants were kept for the analyses: 7
113 young controls ([2 females], age=31±7 yo), 4 older controls ([1 female], age=72±2 yo), and 16 drusen
114 patients ([10 females], age=74±4 yo). Their demographic and ophthalmological characteristics are
115 given in **Table 1**.

116 All clinical, experiment, and data management procedures were approved by the Ethical
117 Committee "CPP Ile de France V" (ID RCB 2015-A01094-45, n. CPP: 16122 MSB), and they adhered
118 to the tenets of the Declaration of Helsinki. A signed consent was signed by each participant to be
119 included in the study as well as for the inclusion in the Multimodal Ophthalmologic Imaging protocol
120 (IMA-MODE, ID_RCB 2019-A00942-55 CPP: Sud Est III 2019-021-B) of the Quinze-Vingts National
121 Ophthalmology Hospital.

122 **Drusen detection by gaze-dependent imaging**

123 In order to reliably detect the presence of even the smallest drusen, gaze-dependent fundus
124 imaging of all older participants' central retina was performed using a commercial clinical-grade AO-FIO
125 (rtx1, Imagine Eyes) following the method and protocol described by Rossi et al.[16]. Compared to direct
126 single-shot retinal flood imaging, gaze dependent imaging computes the local maxima of contrast
127 across a stack of 5 images whose gaze direction has been sequentially shifted: one 4°x4° fovea-
128 centered image of the retina, focused on the photoreceptors, and four 4 horizontally and vertically

displaced images (±1° with respect to the center image). After image registration, the maximum of the standard deviation for each x, y pixel of the 5-image stack is computed to make gaze-varying structure visible. In the resulting contrast image, drusen and their delineation are clearly visible (**Fig. 2c**). This gaze-dependent retina imaging method allows for the detection of foveal drusen less than 25 µm in diameter that are not detected by standard imaging methods and it also visualizes much more reliably drusen 25-60 µm in diameter, providing more precise information about their size and position[16]. In a final step, drusen were manually annotated as ellipses by two experts in medical images, followed by a validation by two ophthalmologists (including M.P.). All the image filtering, registration, and processing were performed using custom software written in MATLAB (Mathworks, USA, 2023).

Ocular fixation task

Following drusen assessment, all participants were tested in an ocular fixation experiment in order to see whether the presence of drusen affects fixational eye movements. In order to precisely detect even the smallest eye movements, video recordings of the fovea during fixation were performed using the PARIS AO-FIO (ONERA)[17] located at the Quinze-Vingts National Ophthalmology Hospital in Paris, France. Both the PARIS AO-FIO retinal imaging setup and retinal motion tracking process are described in the following sections. Before the ocular fixation task, the dominant was eye dilated with a drop of 1% tropicamide (*Mydriaticum*, tropicamide 0.5%). The recordings were performed in a dark room with minimal stray light and with the participant's head fixed on a chinrest. The fixation task consisted of two phases. In the initial phase, participants were required to fixate a central cross for 5 seconds. This phase served to initialize the retinal motion tracking procedure. In the experimental phase, the participants were asked to fixate a circle (outer diameter: 17 arcmin (0.28°), inner diameter: 11 arcmin (0.18°)) for 30 seconds, across 5 trials. The instructions were *"Please, fixate the circle for 30 seconds. Do not speak and try not moving your head. Do not hesitate to blink if you need to.",* and a vocal indication about time progression was provided after 15 seconds.

Retina imaging setup

High-resolution structural imaging of the fovea was made performed using the PARIS AO-FIO[17], through video recordings focused on the photoreceptor layer. Concurrently with retina imaging, the Paris AO-FIO allowed for the projection of NIR illumination patterns (i.e., stimuli) onto the retina via a

157 deformable Digital Micromirror Device (DMD)[18] as well as for partial-field illumination[19]. The stimulus
158 projection with the DMD was controlled using a custom-made Python code and the ALP4Lib python
159 library wrapper. The PARIS AO-FIO system consists of two optical channels: the Wavefront correction
160 channel, and the illumination and imaging channel, combined with the stimulation channel. A fibered
161 SuperLuminescent Diode (Exalos, Switzerland) with nominal center wavelength of 750 nm measures
162 optical aberrations, and an 850nm LED source (Thorlabs, USA) coupled with a liquid fiber
163 homogeneously illuminate the retina over a 4° diameter field of view (**Fig. 1a**). The adaptive optics
164 compensated for the spherical, cylindrical and some higher order aberrations of the eye's optics before
165 the stimulus reached the retina. The backscattered light from the eye was reflected back on the
166 deformable mirror before reaching the imaging camera. The adaptive optics loop was controlled with a
167 LabVIEW program and image acquisition was monitored via the Holovibes software[20].

168 **Retina motion tracking**

169 During the initial phase of the ocular fixation task (5s), a full field sequence of images covering
170 a 4° diameter field of participants' retina was recorded at 100 Hz (2048 x 2048 pixel frames). The
171 recorded full field retinal images were first stabilized and then averaged into a unique squared full field
172 reference image of the center of the retina (**Fig. 1a**). Then, during the experimental phase of the task,
173 only a sub-band (2° x 0.5°, 1400 x 256 pixel, with the black circle target at the center) was recorded at
174 800 Hz to be used for retina motion tracking (**Fig. 1b**). Retinal motion was tracked using a phase-
175 correlation registration method[21,22] (**Fig. 1c**) after bandpass filtering the image sequences. The
176 algorithm consisted in finding the position that best fitted each frame of the high-speed video onto the
177 reference image. The best fit was considered as the peak value coordinates of the correlation map
178 computed in the Fourier domain. See **Clip 1**.

179 Even if the maximum sampling frequency of the camera was only limited by vertical pixel
180 resolution, we found that 1400-pixel horizontally offered a good tradeoff between field coverage and
181 video bandwidth. The resulting 0.684 MB/frame (16 bits) led to a very large 547 MB/s video bandwidth
182 that could only be recorded with solid state hard drives and ad-hoc recording software (Holovibes).
183 Videos were recorded on a separate computer than the one used for stimulus presentation.

184 **Detection of retina motion related events**

185 Processing of the raw pixel displacement of each frame relative to the reference images to
186 ocular movement in arcminutes with annotated events was made with a MATLAB custom program
187 (based on the work of Bowers and Gautier[23]). Microsaccades were detected using an acceleration
188 threshold inspired by Engbert[24]. An acceleration, rather than velocity, threshold (factor N=3 standard
189 deviation of the median) was used in order to differentiate fast ocular drift epochs from small and slower
190 microsaccades which can have similar velocities but distinct accelerations. The acceleration was
191 computed for the 30 s fixation, and smoothed using running average with a 70~ms window. This
192 adaptive algorithm allowed for thresholds that fitted the participants who had relatively small
193 microsaccades and stable ocular drift, as well as the participants with larger microsaccade and drift
194 amplitudes. In addition, to ensure that microsaccades were all entirely detected and that some parts of
195 ocular drift were not mislabeled as microsaccades, all traces were manually verified after the automatic
196 annotation. Blinks were detected automatically as sudden drops in mean frame pixel intensity, which
197 corresponded to the closed eye reflecting less light back to the camera. Rejected data were epochs of
198 ocular coordinates marked by the user as false data due to failures in the imaging or the tracking (to
199 the exclusion of blinks). They accounted for 0-3% of the fixation data for each participant. Everything
200 in-between the three types of events – microsaccades, blinks or rejected data – was automatically
201 marked as drift.

202 Root mean square sample to sample (RMS-S2S) deviation was calculated to measure the
203 precision of the retina tracking method. A given RMS-S2S of an eye-tracker quantifies the average
204 movement due to noise between successive data is its squared value[25,26]. Filtering ocular traces can
205 have a strong effect on RMS-S2S and skews the results[27]. However, in this tracking method, ocular
206 traces were used raw, and RMS-S2S appeared to be the right metric to measure precision.

207 **Estimation of fixation stability**

208 The Bivariate Contour Ellipse Area (BCEA) and, more recently, the ISOline Area (ISOA) metrics
209 have been used to clinically measure fixation stability of patients with central vision loss, including
210 AMD[28]. ISOA is more robust than BCEA as it can delineate non-ellipsoidal fixation patterns[29] and it can
211 be used to detect possible multiple retinal fixation loci (PRLs), such as in AMD patients. The choice of

212 the bandwidth and the extent (i.e., number of standard deviations) to compute the ISOA is relatively
213 arbitrary and open to criticism[29–31]. The choice of a 1° window for kernel density estimation, which
214 subtends ISOA calculation, has been shown to be robust and appropriate with respect to the classical
215 definition of the 1° foveola[30,31]. Concerning the ISOA contour extent, we used both the standard 68%
216 ISOA (i.e., encompassing 68% of the data points) and the 86% ISOA (i.e., computed over 2 standard
217 deviations in the 2D space defined from the center of the fixation distribution[32]. The rationale was that
218 the 86% ISOA contour would provide complementary insights on the global fixation pattern that might
219 better differentiate healthy controls from participants with foveal drusen.

220 **Drift diffusion coefficient and amplitude spectrum computation**

221 In the framework of Brownian motion[33,34], the eye movement during drift epochs can be
222 modeled by a random walk, and motion statistics can be measured by the diffusion coefficient *D*. We
223 computed the diffusion coefficient *D* by least square best fit to the measurements of the empirical
224 standard deviation of the eye displacement as a function of time[35]. The motion amplitude spectra of the
225 ocular drift segments were analyzed by using a multitaper spectral analysis. This analysis was carried
226 separately on the horizontal and vertical components of eye motion[36,37], on overlapping segments of 1
227 s. The time half-bandwidth product was fixed at 2.5, and the last taper was dropped to maximize spectral
228 concentration ratios in the Slepian sequences.

229 **Results**

230 **Detection and characterization of foveal drusen**

231 **Figure 2** shows foveal drusen detected in one participant by using gaze-dependent retinal
232 fundus imaging protocol[16] (**Fig 2c)**, as well as the corresponding region in an SD-OCT cut across the
233 fovea (**Fig 2a-b**). Overall, in 9 out of 20 participants (45%), initially deemed to have no drusen and
234 therefore assigned to the control group based on SD-OCT images, the presence of foveal drusen was
235 detected using the gaze-dependent detection procedure. These participants were therefore reassigned
236 to the drusen group (see Methods). Across all participants of the drusen group, we quantified the
237 number of foveal drusen, their eccentricity with respect to the center of the fovea, their areas, their
238 diameters (i.e., computed as the average diameter of the ellipses), and the total area covered by all
239 drusen (**Table 1**). The median drusen diameter in the study was 60 µm (0.2°) (**Fig 2e**).

240 **Precision and robustness of retinal motion tracking**

241 Retinal tracking during ocular fixation was performed using the Paris AO-FIO[17] as described in
242 Methods. **Figure 3** shows the example traces recorded during 4s of the ocular fixation task in one
243 control participant and one participant with ocular drusen. Our retinal tracking method allowed both
244 microsaccades (shown in magenta) and ocular drift (shown in blue) to be easily visualized and detected
245 in both control and drusen participants.

246 The precision of the tracking procedure was quantified by the average RMS-S2S and achieved
247 0.0015°, as measured on unfiltered data across all participants. This value is an order of magnitude
248 lower than what is deemed sufficient to detect microsaccades by Holmqvist[25] (0.03°). A low standard
249 deviation of the tracking error (σ=0.0006°) suggests that the method is very robust from participant to
250 participant. Finally, in order to assess possible noise sources stemming from either mechanical vibration
251 of the Paris AO-FIO setup or defects of the tracking algorithm, as well as to get a standard RMS-S2S
252 value, we quantified the precision of the tracking method on non-moving artificial eye (OEMI-7 Ocular
253 Imaging Eye Model). We found an RMS-S2S of 0.00019° (σ=0.00009° over 4 recordings). The precision
254 found on human eyes and the artificial eye is equal or better than any reported values in literature
255 (0.0069° on a DPI Gen5.5 with an non-moving artificial eye[38] and 0.012° on a human eye[39]; 0.0012-
256 0.0045 on the EWET1 prototypes on human eyes[39]) without being affected by lens-wobble artifacts
257 such as in a DPI or distortion artifacts such as in an AO-SLO system (no RMS-S2S values found for
258 AO-SLO in literature).

259 The sensitivity to noise was additionally assessed by power spectrum analysis. Power spectra
260 were only weakly affected by noise across all subject groups, even at higher frequencies (above 100Hz,
261 **Figs 5c,d**). The power spectrum of the still model eye was one to two orders of magnitude below human
262 participants (**Supp. Fig. 1**), suggesting negligible setup-related noise.

263 An addition to be very precise, the method was also found to be resistant to variations in lens
264 transparency (**Supp. Fig. 2**). More specifically, in 11 participants (41%), classified by orthoptists as
265 having corticonuclear lens opacities, the mean RMS-S2S was 0.0018°, only slightly superior to the
266 mean RMS-S2S of all other participants (0.0014°).

267 **Effect of eccentricity of foveal drusen on microsaccades**

268 To see whether the presence of foveal drusen is associated with changes in eye movements,
269 we plotted individual distributions of microsaccade amplitudes sorted from lowest to highest mean
270 amplitude (**Fig 4a).** The distributions of young and older participants from the control group were shifted
271 toward the lowest amplitudes, whereas those from the drusen group towards the highest ones,
272 suggesting a link between drusen properties and FEM characteristics. Strikingly, we also noted that the
273 highest microsaccade amplitudes were associated with the presence of drusen mainly inside the
274 foveola (the 0.4-0.6° foveal pit)[40], suggesting that drusen eccentricities may play an important role in
275 oculomotor changes induced by the presence of drusen.

276 To quantify this effect, we computed Pearson's correlation coefficients between the measured
277 drusen characteristics (i.e. their number, area and eccentricity) and microsaccade sizes. We found a
278 significant negative correlation between the participants' drusen eccentricities and their microsaccade
279 amplitudes (r=-0.74, p=0.001). Hence, the closer drusen were to the center of the fovea, the larger were
280 microsaccades. Conversely, the more eccentric were the drusen in a particular participant, the more
281 similar this participant was to the control subjects in terms of the microsaccade amplitude. No significant
282 correlation was found between the number of drusen, the mean drusen area or the total drusen area
283 and microsaccade amplitude (r=-0.003, p=0.99; r=0.16, p=0.53; r=0.13, p=0.61, respectively. The
284 results in **Fig. 4b** show that microsaccade amplitudes start increasing exponentially when drusen are
285 located closer than 0.8°-1° with respect to the center of the fovea.

286 To further characterize the role of drusen eccentricity, participants from the drusen group were
287 subsequently classified into two subgroups. The classification took into account the approximate
288 diameter of the foveola (0.4-0.6°[40]), of the stimulus (0.28°), and of the median foveal druse (0.2°). The
289 first subgroup (named DIF, for "drusen inside the foveola") included the participants with drusen mainly
290 located in the foveola (i.e., mean drusen eccentricity less than 1° with respect to the center of the fovea,
291 n=8). The other subgroup (named DOF, for "drusen outside the foveola") consisted of participants with
292 drusen located mainly outside their foveola (n=8).

293 Statistical analysis using linear mixed effects model revealed significant differences between
294 the microsaccade amplitude in the DIF group and the three other groups (**Fig. 4c**; DIF vs young controls:

295 |t|=6.5, p=10^{-9}; DIF vs older controls: |t|=6, p=10^{-9}; DIF vs DOF: |t|=5, p=10^{-7}). The group with drusen
296 outside the foveola (DOF) tended to have larger microsaccades than young controls (|t|=1.7, p=0.09)
297 and older controls (|t|=1.8 p=0.06). There was no difference between young and older controls (|t|=0.4,
298 p=0.66).

299 While no significant differences were found between groups in terms of *average* drusen area,
300 we hypothesized that large drusen closer to the center of the fovea should have an even stronger effect
301 on microsaccade amplitude. The rapid drop-off of both cone density and acuity in the fovea suggest
302 that both drusen area and eccentricity can have tremendous effect on foveal vision. We therefore
303 computed the correlation between drusen area divided by eccentricity (that we called drusen density)
304 and measured FEM characteristics. This new measure was indeed stronger correlated with
305 microsaccade amplitude (r=0.82, p=0.0001) than the eccentricity alone.

306 The above results show that drusen eccentricity, a simple property of retinal structure
307 associated with presymptomatic stage of AMD, is a crucial factor explaining the difference in
308 microsaccade size between control participants and subjects with a relatively elevated risk of
309 developing the disease. The quality of this simple structural measure in explaining functional changes
310 can be further improved by taking into account drusen area.

311 **Impact of foveal drusen on ocular drift and eye motion spectrum**

312 Apart from microsaccades, the ocular drift component of FEM (see **Fig. 3**) was also affected by
313 the presence of foveal drusen, but to a lesser extent. Indeed, the analysis of ocular drift in the four
314 participant groups defined in the previous section revealed significant differences in drift diffusion
315 coefficients between participants with drusen in the foveola and control subjects (**Figs. 5a,b**; DIF vs
316 young controls: |t|=2.5, p=0.01; DIF vs older controls: |t|=2, p=0.04). Statistical pairwise comparisons
317 between all other groups have shown that the DOF group was significantly different from young controls
318 (|t|=2, p=0.04), but not from older controls (|t|=1.7, p=0.1). No differences were found between young
319 and older controls (|t|=0.1, p=0.93). Individual diffusion coefficient revealed larger variability within
320 groups but less between groups (**Fig 5a,b**) when compared to mean microsaccade amplitude (**Fig 4a**).
321 No significant correlations were found between drift diffusion coefficient and drusen properties across

322 all subjects (eccentricity: r=0.09, p=0.72; drusen number: r=-0.003, p=0.99; mean drusen area: r=-0.1,
323 p=0.69; total drusen area: r=-0.05, p=0.85)

324 A different way to analyze FEM changes induced by drusen presence is look at the motion
325 spectrum across the subject groups. The spectral analysis of ocular drift revealed a progressive
326 increase in motion amplitude both with age and drusen centrality (**Fig. 5c**), marked in the middle
327 frequency range (10-40 Hz). No difference in motion amplitude was observed at high frequencies (100-
328 400 Hz) between the two drusen groups, in contrast to an age-related difference in control subjects
329 (**Fig. 5c**). When accounting for the spectral changes caused by microsaccades (**Fig. 5d)**, the foveolar
330 drusen group clearly stood out across all motion frequencies, potentially impeding later-stage neural
331 processing of the visual input[35]. The differences between the two motion spectra (**Fig. 5c,d)** reflect the
332 statistical differences in drift diffusion coefficient between subjects groups presented above and
333 highlight the more important role of microsaccades, compared to ocular drift, in FEM changes induced
334 by the presence of central drusen.

335 **Foveolar drusen impair fixation stability**

336 Fixational micromovements of the eye, including microsaccades and drift, are the primary
337 determinants of fixational stability, a functional measure of ocular stability at the macroscopic level
338 usually evaluated by such measures as ISOline Area[28,29] (see Methods). The discovered relationship
339 between central drusen and microsaccade size, described in the previous section, suggests that a
340 similar relationship should exist between drusen eccentricity and ocular stability in the fixation task.
341 Indeed, we found a strong and significant negative correlation between ISOA (at 86% level) and drusen
342 eccentricity (r= -0.72, p=0.001) as well as highly significant positive correlation between ISOA and
343 drusen density (r= 0.72, p=0.0004 across all subjects. We checked that there were no significant
344 differences between participants in terms of microsaccade frequencies that could explain changes in
345 fixation stability.

346 In order to better understand the effect of drusen on fixation stability and its topological
347 characteristics, we quantitatively compared average ISOA values across the four groups of subjects
348 using linear mixed modeling approach and visualized average ISOA contours. The participants with
349 drusen mainly in the foveola had the largest ISOA as compared to the other three groups (DIF vs young

350 controls: |t|=5.5, $p=10^{-7}$; DIF vs older controls: |t|=4.9, $p=10^{-6}$; DIF vs DOF: |t|=5.4, $p=10^{-7}$). ISOAs
351 remained similar between the DOF group and young controls (|t|=0.24, p=0.81) or older controls
352 (|t|=0.24, p=0.67), and between young and older controls ((|t|=0.2, p=0.83). These results extend our
353 conclusion from the previous section by showing that impaired fixation stability in subjects with drusen
354 in foveola is primarily mediated by the increase in microsaccade size and not by other FEM properties,
355 such as ocular drift.

356 Previous studies in patients with central scotomas suggest that these patients may develop one
357 or more eccentric areas of fixation (referred to as preferred retinal locus or PRL)[41], giving rise to an
358 extended overall fixation area. We therefore checked in our presymptomatic subjects from the DIF
359 group whether they express increased and possibly multipeaked fixation densities (as opposed to
360 Gaussian-like distributions expected for the other groups). This was indeed the case, as only in the DIF
361 group the ISOA contours exhibited multiple "islands" (**Fig. 6**). While in most of the DIF participants
362 fixation distributions expanded along the horizontal axis, in some participants the area of fixation
363 increased along the vertical axis. We note here that the density compartmentalization effect was evident
364 only for contours encompassing 86% of fixation density, but it was virtually invisible at 68%. Such a
365 density compartmentalization could indicate a possible initial step towards forming multiple PRLs with
366 further progression of the disease. Indeed, high-resolution video recordings of fixation dynamics in
367 subjects with central drusen (see **Clip 2**) allow us to speculate that the oculomotor system can adapt
368 itself to the presence of a single drusen (at least in the foveolar region), and evolve accordingly as their
369 number and size increase. This suggestion however requires a more careful future study.

370 Given the consistent and strong effect of foveal drusen on both fixation stability and
371 microsaccade amplitude, it is not surprising that there was a strong correlation between the ISOA 86%
372 values and microsaccade amplitudes across the entire study population (**Fig. 7a**; $r^2=0.85$, p=0.001).
373 Interestingly when looking at figure 6, in all groups except DIF, higher values for ISOA seemed to come
374 with both proportional increases in microsaccade amplitude and drift diffusion coefficient at the same
375 time. However, for the DIF group, drift diffusion coefficient appeared to lose its correlation with ISOA
376 compared to the rest of the study population (**Fig. 7b**), while still following the same linear correlation
377 for microsaccade amplitude (**Fig. 7a**). That could be interpreted as fixation instability being primarily
378 caused by larger microsaccade in DIF participants and less because of drift. That is consistent with the

379 analysis of the motion power spectra in the previous section. Moreover, the data points were clearly
380 clustered together around higher values of both ISOA and microsaccade amplitudes (red data points in
381 **Fig. 7**), suggesting the possibility of automatic detection procedure for the existence of foveolar drusen
382 that could for instance use both ISOA and microsaccade amplitude values.

383 **Discussion**

384 The objective of the present study was to see whether structural retinal changes in
385 presymptomatic AMD can have detectable consequences on functional aspects of vision. More
386 specifically, we tested the hypothesis that FEM abnormalities are associated with early structural retinal
387 anomalies, such as the appearance of small central drusen.

388 The primary finding of this study is that participants with foveal drusen exhibit significantly larger
389 microsaccades and higher fixation instability (measured by ISOA) as compared to healthy controls,
390 while maintaining equivalent microsaccade rates. Strikingly, drusen eccentricity with respect to the
391 center of the fovea appears to be the main determinant factor associated with larger microsaccades
392 and ISOAs. Indeed, we found that the more central the drusen were, the more unstable the fixation
393 was; conversely, the further from the center of the fovea the drusen were, the more the participants
394 tended to behave like controls, with minimal to no changes in fixation stability. We propose the following
395 quantification criterion to assess the point after which drusen eccentricity strongly affect fixation
396 characteristics: Microsaccade amplitude starts increasing exponentially when average drusen
397 eccentricity is less than 1° with respect to the center of the fovea. Considering the size of the typical
398 drusen and of the fixation target, the threshold point approximately corresponds to the size of the
399 foveola, i.e. the 350 μm foveal pit as defined by Kolb[40]. Our results further suggest that quantification
400 of microsaccade amplitude and ISOA in a simple ocular fixation test could in principle be sufficient to
401 discriminate healthy participants from those with retinal anomalies in the foveola, such as drusen.

402 In this study, we also evaluated the impact of foveal drusen density and eccentricity on the
403 ocular diffusion drift coefficient, which provides a displacement estimator reflecting the randomness and
404 stability of visual fixation[35]. The motion spectrum of drift epochs without microsaccades appeared
405 however impacted by the presence of drusen and their centrality, especially in the middle frequency
406 range. The dynamics of the complete eye movements (i.e. microsaccades included) during fixation

407 appears successively altered with age, with the presence of foveal and further with foveolar drusen.
408 This confirms the impact of drusen on microsaccade dynamics, and the importance to finely
409 characterize them. Further research is needed to understand the role and implication of drusen on
410 visual sampling and perception.

411 Another interesting observation stemming from this study concerns the definition of *healthy*
412 *older adults* from an ophthalmological point of view. Twenty participants of this study were initially
413 recruited as healthy controls based on the fact that (i) no visible foveal drusen were found using
414 standard SD-OCT imaging analyzed by ophthalmologists, and (ii) no visual symptoms (in terms of visual
415 acuity, contrast sensitivity, and so on) were observed during inclusion to the Silversight cohort.
416 Subsequently, using AO-FIO-based gaze-dependent retina imaging, 45% of these participants were
417 found to actually have small drusen in their fovea. This experimental observation, made with the use of
418 more advanced imaging technique, aligns with early studies suggesting that drusen are more prevalent
419 than previously assumed[42,43]. It also emphasizes the utmost importance of the development of sensitive
420 measurement techniques that can be applied at presymptomatic stages to detect the presence of small
421 drusen. While recent progress in retinal imaging resulted in retromode[44] or gaze-dependent[16] methods,
422 which can both detect drusen invisible in standard SD-OCT images, this study opens up a new avenue
423 in drusen detection research by showing that the appearance of small drusen can be detected based
424 on simple functional measures, i.e. by looking at the FEM. Moreover, the discovered link between
425 central drusen and fixation stability can explain the discrepancy present in the literature regarding the
426 differences in fixation stability between young and healthy older adults, with some studies reporting an
427 age-related decrease in stability[45–47] and other studies, including ours, reporting no effect of age[48–50]. If
428 the presence of foveal drusen is a common trait among older participants and these drusen do affect
429 fixation stability, as we observe in our experiment, then the putative effect of age on fixation stability in
430 the above studies can in fact be explained by the presence of participants with undetected central
431 drusen in the sample of older adults (since virtually all previous studies used standard retina fundus
432 imaging or SD-OCT). In conclusion, a combination of imaging methods and functional oculomotor
433 measures, with a potential addition of subjective patient-reported measures of retinal health[50] can be
434 part of the general strategy for multifactor screening for retinal diseases, including AMD, in the general
435 population. While it is currently impossible to know whether or not existing drusen will develop into
436 severe forms of AMD[51], detection of drusen at the earliest possible stage will allow to monitor their

437 progression and take the necessary precautions (e.g. apply anti-VEGF treatment[4]) before critical and
438 irreversible damage occurs. Health style changes might help slow down their growth, and new drugs
439 are currently being clinically tested to prevent the formation and evolution of drusen[7].

440 To the best of our knowledge, alterations of fine oculomotor control in relation to small,
441 asymptomatic changes of retinal structure have never been previously reported, whereas the
442 assessment of eye movements to identify non-invasive biomarkers of a number of diseases is not
443 new[52]. Research on eye movements has indeed existed for more than a century, and infrared video eye
444 trackers capabilities, accuracy, and accessibility have renewed the interest on eye movements to
445 clinicians and psychologists. FEM have been explored in neurological disorders such as amblyopia[53,54],
446 schizophrenia[55], Parkinson's disease[56], and others[57]. There have also been attempts to reveal new
447 FEM-based biomarkers to predict multiple sclerosis and follow its progression[58]. However, when it
448 comes to detecting subtle retinal structural anomalies by means of FEM analysis, it is key to be able to
449 record the whole spectrum of microsaccade amplitudes, down to 1 arcminute. The recent use of
450 adaptive optics retinal imaging instruments has made it possible to reach this resolution. The AO-FIO
451 used in this study allowed us to observe an average healthy microsaccade amplitude of 6.3 arcminutes,
452 whereas participants with drusen had an average microsaccade amplitude of 13.8 arcminutes. In the
453 past 20 years, FEM studies using pupil-based eye trackers have defined a microsaccade with
454 amplitudes up to 1-2°[25,59–61], and basic fixation tasks often showed average microsaccade amplitudes
455 of 20-60 arcminutes. It is thus possible that the differences between controls and drusen participants
456 found in our study would not have been detected using these less precise eye trackers and/or a fixation
457 target larger than ours, because microsaccade amplitude is known to be target-dependent[23].

458 While general functional significance of microsaccades is still a matter of debate, many
459 researchers agree that microsaccades play an important functional role in the presence of foveolar
460 stimuli, and the foveola size is even considered as a reference to define microsaccades[59,62]. As
461 discussed in Poletti's review on attention and eye movements at the foveal scale[59], any stimuli in the
462 foveola can be attention-grabbing and whether it is voluntary or not, it is possible to have microsaccade
463 directed towards different stimuli as close as 20 arcminutes from each other. It would not be correct to
464 consider foveal drusen as inputs to the visual system, but our data suggest that they might change
465 retinal processing in specific retinal locations. Drusen appears to distort foveal vision but the exact role

of or consequence on the oculomotor system remains to be determined. Fixation instability could be the result of the oculomotor system adaptation to avoid drusen locally. The second hypothesis consists in a more widespread RPE/photoreceptor dysfunction and degraded foveal sensory integration which would in turn impair motor control. The local compensatory versus global oculomotor deficiency hypotheses require further investigation. The relative impact of each eye's drusen on binocular vision is another open subject of research to supplement these findings.

In conclusion, by combining state-of-the-art retinal imaging techniques and novel retinal motion tracking approach, we report an association between the presence of foveal drusen and fixation instability, hence linking structural and functional changes during aging. This study demonstrates a strong association between foveal drusen properties and oculomotor behavior in a simple ocular fixation task. It may be considered as a functional biomarker candidate for innovative AMD screening approaches. It may also be of interest to document the effect of foveal drusen and its resulting fixation instability on more active tasks such as reading performance or visual search. A longitudinal study could also clarify the joint evolution of fixation instability and drusen progression.

Figures

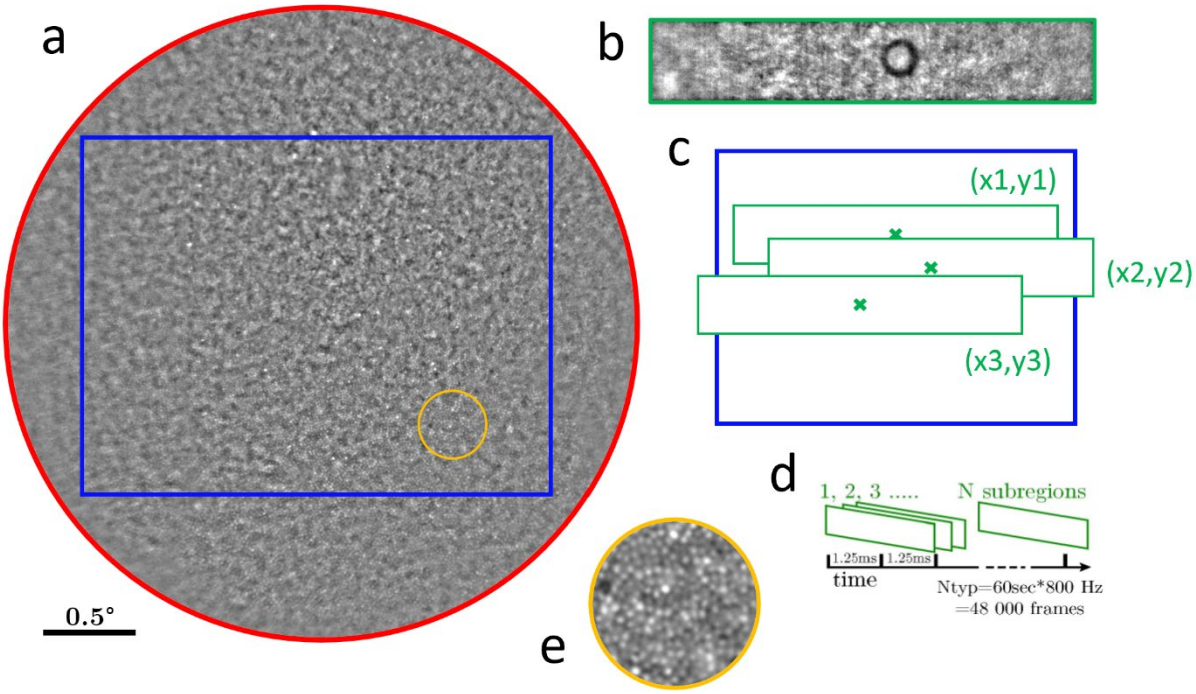

Figure 1. Principle of the AOFIO retinal tracking. (a) The 4° full field obtained after initial phase of the fixation task (5 sec at 100 Hz, in red). Only the rectangular sub-part (in blue) was used as a reference image for subsequent eye movement analysis, as it is enough to track and monitor eye movements during central fixation (typically less than 2° in amplitude). During the experimental phase of the task, the 2 x 0.5° subregion (in green) is tracked at very high speed (800 Hz, 16 bits). (b) An actual frame recorded at this frequency. (c) Eye displacement is obtained by phase-correlation over the reference image. (d) Custom eye tracking software processes large sequences of up to 5 Mbits/frame. (e) A 3x zoom on an area 1° away from the fovea with clearly visible photoreceptor mosaic.

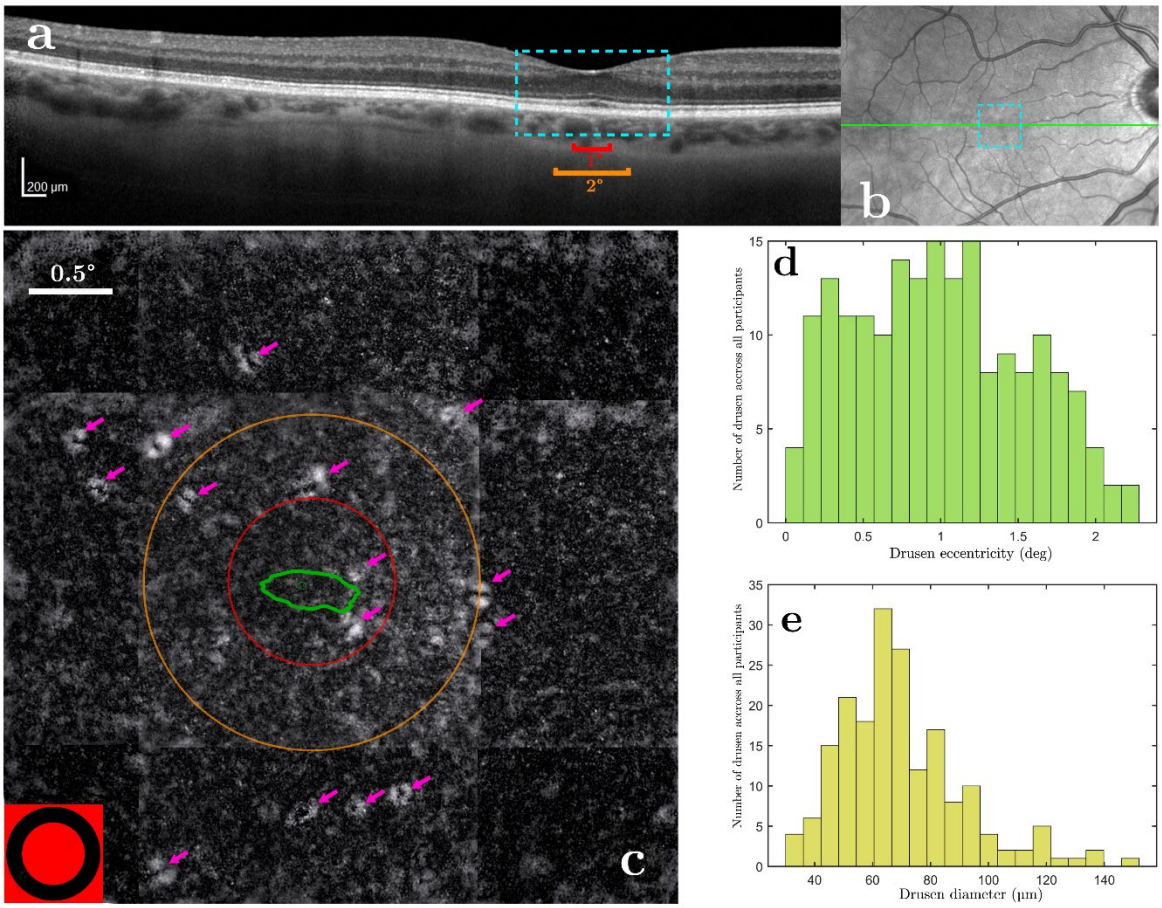

Figure 2. Drusen visualization and identification. (a) SD-OCT image of a patient. A 2x zoom on the 4° center area is shown in blue. The red and orange lines are the same size as the circle diameters in (c). **(b)** Fundus image with the OCT cut of (a) in green and the blue dotted area showing the 4° zone where gaze-dependent imaging is performed. **(c)** Gaze-dependent image of the 4°x4° zone around the fovea of the same patient. Pink arrows indicate the drusen: the white ring is the slope of bump cause by the druse the while the black center part is the tip. The red and orange circles are respectively of 0.5° and 1° of radius. The green line is the ISOA 86% On the bottom left corner the fixation target to scale. **(d-e)** Distribution of drusen eccentricities (c) and diameters (d) across all participants.

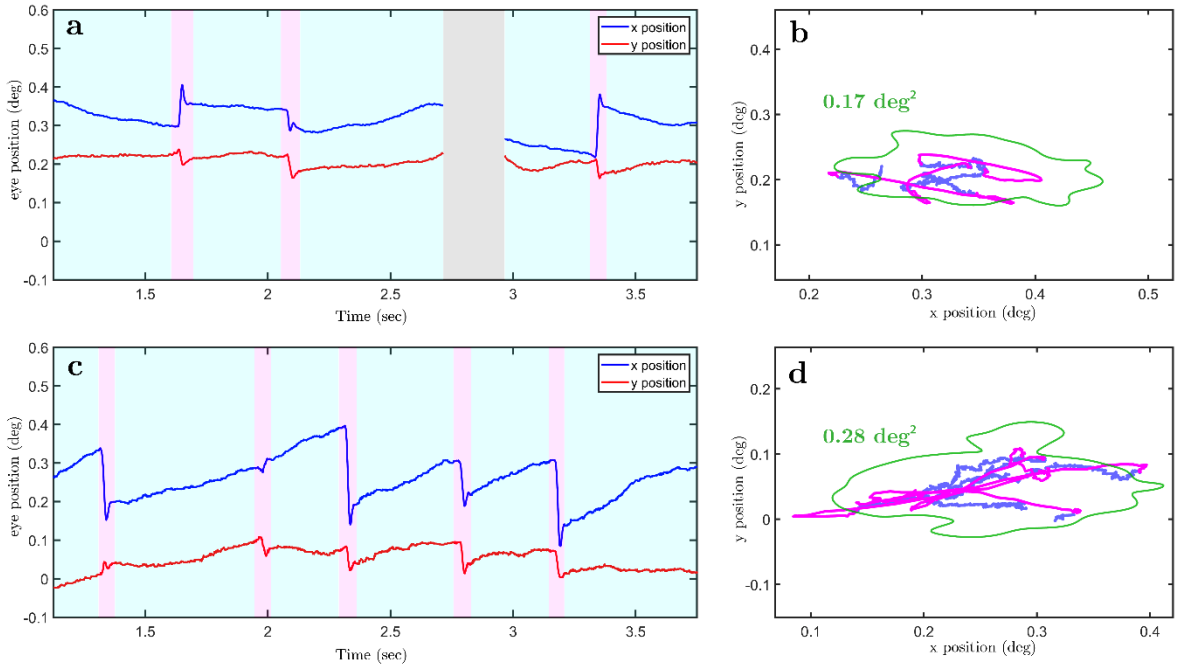

Figure 3. Retina motion traces of a healthy young subject (a-b) vs a subject with drusen (c-d) with the corresponding movement in the visual field. The eye traces are shown for 3 seconds. Microsaccades are annotated in pink and drift in light blue. Eye position is shown in degrees. The green line is the ISOA 86%.

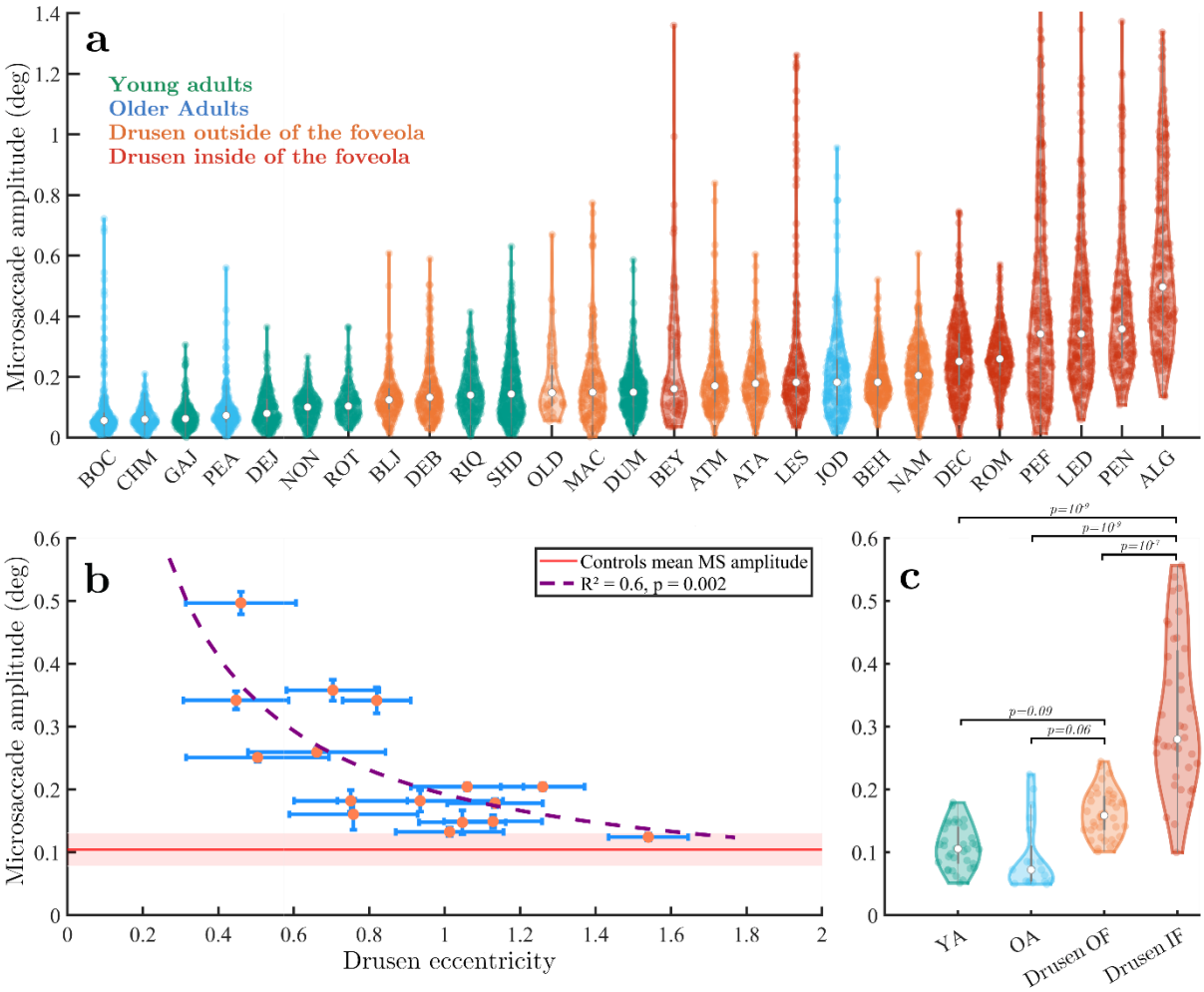

Figure 4. Microsaccade characteristics across individuals and groups. **(a)** Violin plots of individual distributions of microsaccade amplitudes across all participants, color-coded by group and sorted with respect to the mean microsaccade amplitudes. Each dot is one microsaccade during the fixation task. **(b)** Microsaccade mean amplitude with respect to drusen eccentricity from the center of the fovea. Standard errors are shown in blue bars. **(c)** Microsaccade amplitudes across all four groups. Each dot is one trial.

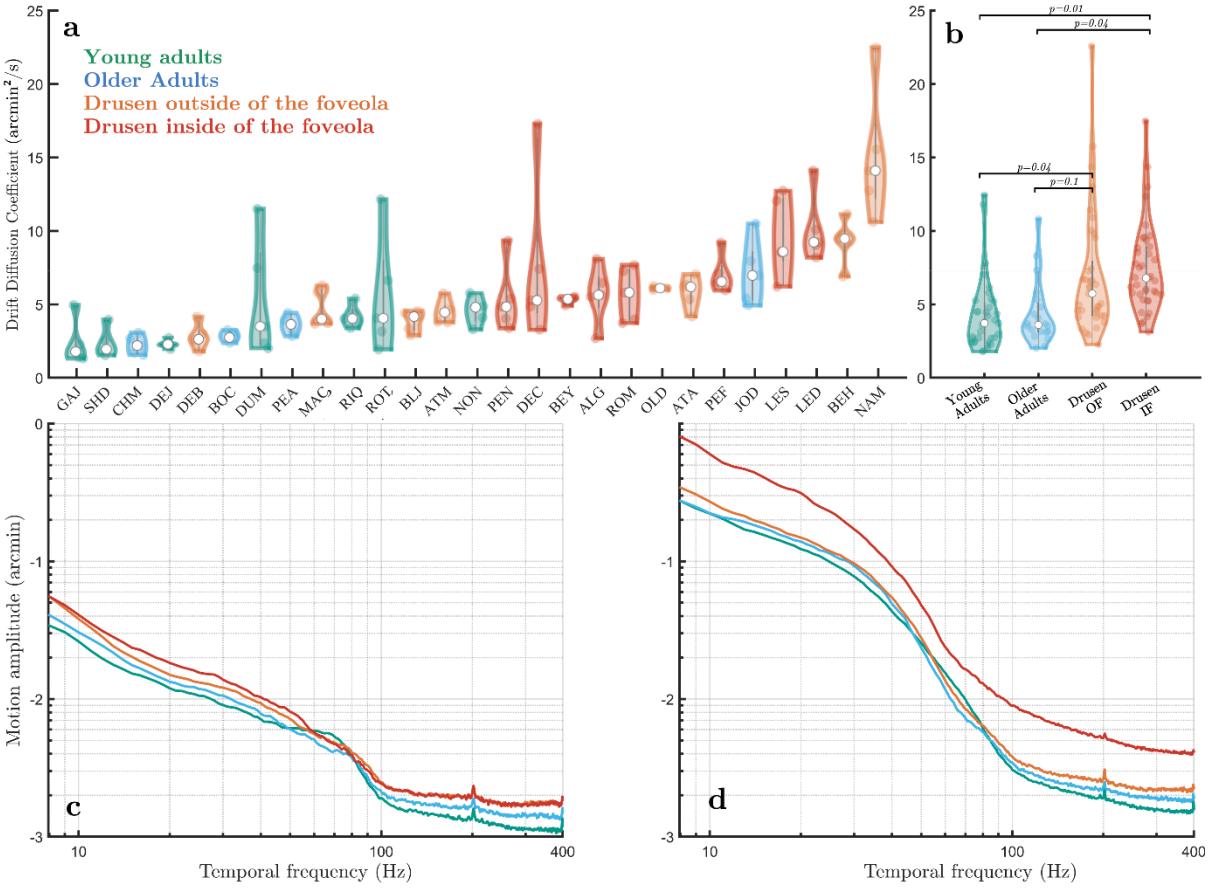

Figure 5. Drift dynamics and motion spectra across groups – horizontal motion. **(a)** Drift diffusion coefficient distribution across all participants, sorted from lowest to highest. Each dot is one trial. **(b)** Drift diffusion coefficient across groups **(c)** Motion spectrum of drifts only across the four groups. **(d)** Whole motion spectrum (drifts + microsaccades) across the four groups. An increase in dynamic across most frequencies is visible with age, and even further with the presence of foveal or foveolar drusen. This progressive increase is particularly visible in the Mid-frequency (10-40 Hz, top left inset) and very-high frequency range (100-400 Hz, top-right inset).

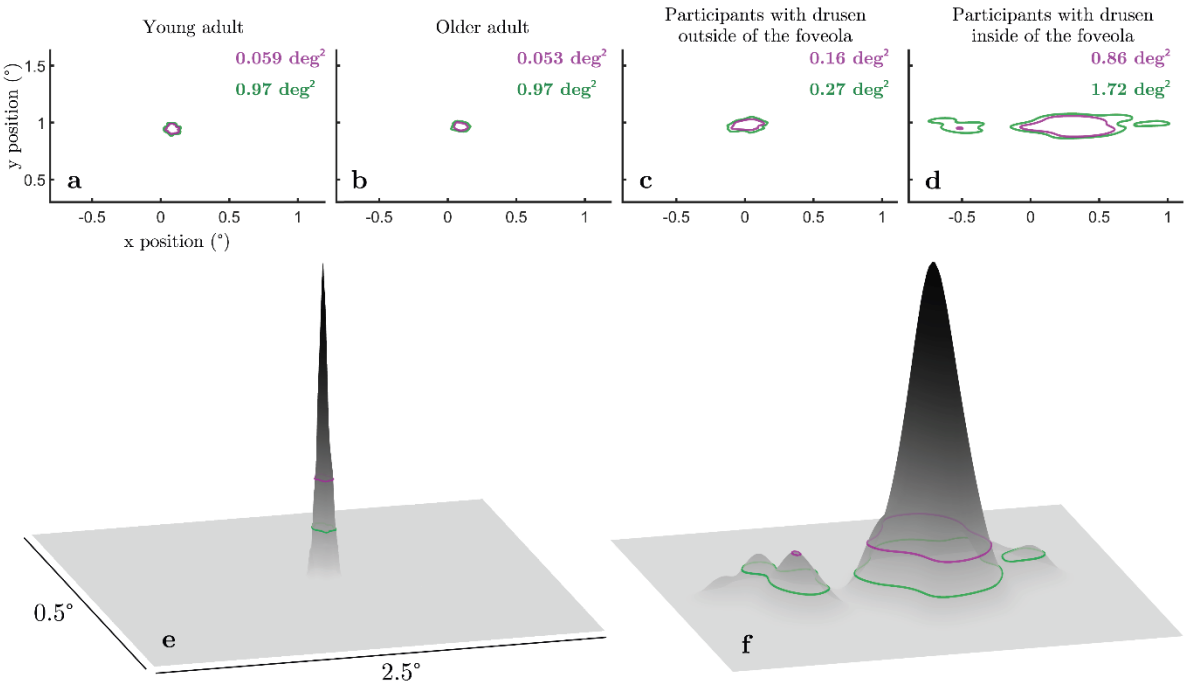

Figure 6. Impact of drusen on fixation stability. (a) The top row shows sample data respectively from a young adult, an older adult, a participant with foveal drusen and a participant with foveolar drusen. **(b)** Probability density of the young adult participant of (a) on the left and the foveolar participant of (a) on the right. ISOA contours encompassing 68% (purple) and 86% (green) of the eye position data.

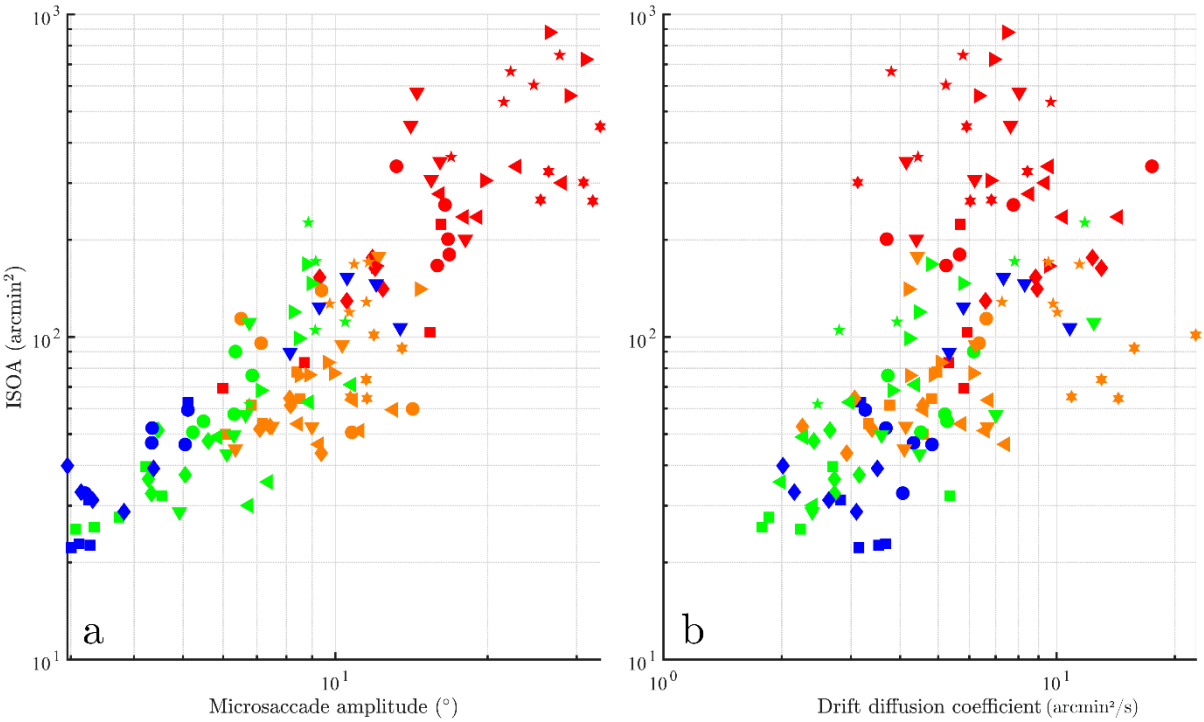

Figure 7. Contribution of microsaccade amplitude and drift coefficient to fixation stability. (a) Microsaccade amplitude vs. 86% ISOA. **(b)** Drift coefficient vs. ISOA on the right. One symbol represents one trial of a participant from its colored group.

534 **References**

535 1. Wong WL, Su X, Li X, et al. Global prevalence of age-related macular degeneration and disease burden projection for 2020
536 and 2040: a systematic review and meta-analysis. *The Lancet Global Health*. 2014;2(2):e106-e116. doi:10.1016/S2214-
537 109X(13)70145-1

538 2. Danis RP, Lavine JA, Domalpally A. Geographic atrophy in patients with advanced dry age-related macular degeneration:
539 current challenges and future prospects. *Clin Ophthalmol*. 2015;9:2159-2174. doi:10.2147/OPTH.S92359

540 3. Pugazhendhi A, Hubbell M, Jairam P, Ambati B. Neovascular Macular Degeneration: A Review of Etiology, Risk Factors,
541 and Recent Advances in Research and Therapy. *Int J Mol Sci*. 2021;22(3):1170. doi:10.3390/ijms22031170

542 4. Rofagha S, Bhisitkul RB, Boyer DS, Sadda SR, Zhang K. Seven-Year Outcomes in Ranibizumab-Treated Patients in
543 ANCHOR, MARINA, and HORIZON: A Multicenter Cohort Study (SEVEN-UP). *Ophthalmology*. 2013;120(11):2292-2299.
544 doi:10.1016/j.ophtha.2013.03.046

545 5. Cervantes-Castañeda RA, Banin E, Hemo I, Shpigel M, Averbukh E, Chowers I. Lack of benefit of early awareness to age-
546 related macular degeneration. *Eye*. 2008;22(6):777-781. doi:10.1038/sj.eye.6702691

547 6. Schultz NM, Bhardwaj S, Barclay C, Gaspar L, Schwartz J. Global Burden of Dry Age-Related Macular Degeneration: A
548 Targeted Literature Review. *Clinical Therapeutics*. 2021;43(10):1792-1818. doi:10.1016/j.clinthera.2021.08.011

549 7. Fleckenstein M, Keenan TDL, Guymer RH, et al. Age-related macular degeneration. *Nat Rev Dis Primers*. 2021;7(1):1-25.
550 doi:10.1038/s41572-021-00265-2

551 8. Seddon JM. Macular Degeneration Epidemiology: Nature-Nurture, Lifestyle Factors, Genetic Risk, and Gene-Environment
552 Interactions – The Weisenfeld Award Lecture. *Investigative Ophthalmology & Visual Science*. 2017;58(14):6513-6528.
553 doi:10.1167/iovs.17-23544

554 9. Verghese P, Vullings C, Shanidze N. Eye Movements in Macular Degeneration. *Annual Review of Vision Science*.
555 2021;7(1):773-791. doi:10.1146/annurev-vision-100119-125555

556 10. Pondorfer SG, Wintergerst MWM, Gorgi Zadeh S, et al. Association of Visual Function Measures with Drusen Volume in
557 Early Stages of Age-Related Macular Degeneration. *Investigative Ophthalmology & Visual Science*. 2020;61(3):55.
558 doi:10.1167/iovs.61.3.55

559 11. Calabrese A, Bernard JB, Hoffart L, et al. Wet versus dry age-related macular degeneration in patients with central field
560 loss: different effects on maximum reading speed. *Investigative ophthalmology & visual science*. 2011;52(5):2417-2424.

561 12. Macedo AF, Crossland MD, Rubin GS. Investigating Unstable Fixation in Patients with Macular Disease. *Investigative*
562 *Ophthalmology & Visual Science*. 2011;52(3):1275-1280. doi:10.1167/iovs.09-4334

13. Kumar G, Chung STL. Characteristics of Fixational Eye Movements in People With Macular Disease. *Investigative Ophthalmology & Visual Science*. 2014;55(8):5125-5133. doi:10.1167/iovs.14-14608

14. Ağaoğlu MN, Chung STL. Exploration of the functional consequences of fixational eye movements in the absence of a fovea. *Journal of Vision*. 2020;20(2):12. doi:10.1167/jov.20.2.12

15. LAGRENE K, Bécu M, Seiple WH, et al. Healthy and pathological visual aging in a French follow-up cohort study. *Investigative Ophthalmology & Visual Science*. 2019;60(9):5915.

16. Rossi EA, Norberg N, Eandi C, et al. A New Method for Visualizing Drusen and Their Progression in Flood-Illumination Adaptive Optics Ophthalmoscopy. *Translational Vision Science & Technology*. 2021;10(14):19. doi:10.1167/tvst.10.14.19

17. Gofas-Salas E, Mecê P, Petit C, et al. High loop rate adaptive optics flood illumination ophthalmoscope with structured illumination capability. *Applied optics*. 2018;57(20):5635-5642.

18. Krafft L, Senée P, Gofas-Salas E, et al. Multimodal high-resolution retinal imaging using camera-based DMD-integrated Adaptive Optics Flood-Illumination Ophthalmoscope. Published online May 10, 2023. doi:10.1364/opticaopen.22769519.v1

19. Krafft L, Gofas-Salas E, Lai-Tim Y, et al. Partial-Field Illumination Ophthalmoscope: improving the contrast of a camera-based retinal imager. *Applied optics*. 2021;60(31):9951-9956.

20. Atlan M. Ultrahigh-throughput rendering of digital holograms. In: *Imaging and Applied Optics 2018 (3D, AO, AIO, COSI, DH, IS, LACSEA, LS&C, MATH, pcAOP) (2018), Paper DM5F.4*. Optica Publishing Group; 2018:DM5F.4. doi:10.1364/DH.2018.DM5F.4

21. Mecê P. *4D Exploration of the Retina for Adaptive Optics-Assisted Laser Photocoagulation*. PhD Thesis. These de doctorat, Sorbonne Paris Cité; 2018.

22. Mece P, Chen A, Petit C, Mugnier L, Paques M, Meimon S. Real-time optical stabilization of retinal motion at micrometer precision using Adaptive Optics Flood-Illumination Ophthalmsocope. Published online December 28, 2023. doi:10.1364/opticaopen.24907464.v1

23. Bowers NR, Gautier J, Lin S, Roorda A. Fixational eye movements in passive versus active sustained fixation tasks. *Journal of Vision*. 2021;21(11):16. doi:10.1167/jov.21.11.16

24. Engbert R. Microsaccades: a microcosm for research on oculomotor control, attention, and visual perception. In: Martinez-Conde S, Macknik SL, Martinez LM, Alonso JM, Tse PU, eds. *Progress in Brain Research*. Vol 154. Visual Perception. Elsevier; 2006:177-192. doi:10.1016/S0079-6123(06)54009-9

25. Holmqvist K, Nyström M, Andersson R, Dewhurst R, Jarodzka H, Van de Weijer J. *Eye Tracking: A Comprehensive Guide to Methods and Measures*. OUP Oxford; 2011.

26. Holmqvist K, Örbom SL, Hooge ITC, et al. Eye tracking: empirical foundations for a minimal reporting guideline. *Behav Res*. 2023;55(1):364-416. doi:10.3758/s13428-021-01762-8

27. Niehorster DC, Zemblys R, Beelders T, Holmqvist K. Characterizing gaze position signals and synthesizing noise during fixations in eye-tracking data. *Behavior Research Methods*. 2020;52:2515-2534.

28. Whittaker SG, Budd J, Cummings RW. Eccentric fixation with macular scotoma. *Investigative Ophthalmology & Visual Science*. 1988;29(2):268-278.

29. Castet E, Crossland M. Quantifying eye stability during a fixation task: a review of definitions and methods. *Seeing Perceiving*. 2012;25(5):449-469. doi:10.1163/187847611X620955

30. Martinez-Conde S, Macknik SL, Troncoso XG, Dyar TA. Microsaccades Counteract Visual Fading during Fixation. *Neuron*. 2006;49(2):297-305. doi:10.1016/j.neuron.2005.11.033

31. Otero-Millan J, Troncoso XG, Macknik SL, Serrano-Pedraza I, Martinez-Conde S. Saccades and microsaccades during visual fixation, exploration, and search: Foundations for a common saccadic generator. *Journal of Vision*. 2008;8(14):21. doi:10.1167/8.14.21

32. Wang B, Shi W, Miao Z. Confidence Analysis of Standard Deviational Ellipse and Its Extension into Higher Dimensional Euclidean Space. *PLoS One*. 2015;10(3):e0118537. doi:10.1371/journal.pone.0118537

33. Intoy J, Rucci M. Finely tuned eye movements enhance visual acuity. *Nat Commun*. 2020;11(1):795. doi:10.1038/s41467-020-14616-2

34. Microsaccades Keep the Eyes' Balance During Fixation - Ralf Engbert, Reinhold Kliegl, 2004. Accessed July 18, 2023. https://journals.sagepub.com/doi/abs/10.1111/j.0956-7976.2004.00697.x

35. Kuang X, Poletti M, Victor JD, Rucci M. Temporal Encoding of Spatial Information during Active Visual Fixation. *Current Biology*. 2012;22(6):510-514. doi:10.1016/j.cub.2012.01.050

36. Thomson DJ. Spectrum estimation and harmonic analysis. *Proceedings of the IEEE*. 1982;70(9):1055-1096.

37. Babadi B, Brown EN. A review of multitaper spectral analysis. *IEEE Transactions on Biomedical Engineering*. 2014;61(5):1555-1564.

38. Holmqvist K, Blignaut P. Small eye movements cannot be reliably measured by video-based P-CR eye-trackers. *Behav Res*. 2020;52(5):2098-2121. doi:10.3758/s13428-020-01363-x

39. Holmqvist K, Orbom SL, Miller M, Kashchenevsky A, Shovman MM, Greenlee MW. Validation of a prototype hybrid eye-tracker against the DPI and the Tobii Spectrum. In: *ACM Symposium on Eye Tracking Research and Applications*. ACM; 2020:1-9. doi:10.1145/3379155.3391330

40. Kolb H, Nelson RF, Ahnelt PK, Ortuño-Lizarán I, Cuenca N. The Architecture of the Human Fovea. In: Kolb H, Fernandez E, Nelson R, eds. *Webvision: The Organization of the Retina and Visual System*. University of Utah Health Sciences Center; 1995. Accessed October 23, 2023. http://www.ncbi.nlm.nih.gov/books/NBK554706/

41. Duret F, Issenhuth M, Safran AB. Combined use of several preferred retinal loci in patients with macular disorders when reading single words. *Vision Research*. 1999;39(4):873-879. doi:10.1016/S0042-6989(98)00179-5

42. Klein R, Klein BEK, Linton KLP. Prevalence of Age-related Maculopathy: The Beaver Dam Eye Study. *Ophthalmology*. 1992;99(6):933-943. doi:10.1016/S0161-6420(92)31871-8

43. Bressler NM, Bressler SB, West SK, Fine SL, Taylor HR. The Grading and Prevalence of Macular Degeneration in Chesapeake Bay Watermen. *Archives of Ophthalmology*. 1989;107(6):847-852. doi:10.1001/archopht.1989.01070010869032

44. Cozzi M, Monteduro D, Airaldi M, et al. Retromode Imaging Technology for Detecting Drusen-Like Deposits in Healthy Adults. *Ophthalmology Retina*. Published online July 2023:S2468653023003147. doi:10.1016/j.oret.2023.07.012

45. Cutini A, Fragiotta S, Spadea L, et al. Normal values and repeatibility of bivariate contour ellipse area (BCEA) with Microperimeter Mp-1. *Investigative Ophthalmology & Visual Science*. 2014;55(13):169.

46. Agathos CP, Bernardin D, Huchet D, Scherlen AC, Assaiante C, Isableu B. Sensorimotor and cognitive factors associated with the age-related increase of visual field dependence: a cross-sectional study. *AGE*. 2015;37(4):67. doi:10.1007/s11357-015-9805-x

47. Morales MU, Saker S, Wilde C, et al. Reference Clinical Database for Fixation Stability Metrics in Normal Subjects Measured with the MAIA Microperimeter. *Translational Vision Science & Technology*. 2016;5(6):6. doi:10.1167/tvst.5.6.6

48. Kosnik W, Fikre J, Sekulerf R. Visual Fixation Stability in Older Adults. 27(12).

49. González EG, Mandelcorn MS, Mandelcorn ED, Tarita-Nistor L. Effect of Visual Feedback on the Eye Position Stability of Patients with AMD. *Vision*. 2019;3(4):59. doi:10.3390/vision3040059

50. Bécu M. *Impact of Healthy Aging on Spatial Cognition. Spatial Navigation and Gaze Dynamics in Ecological Conditions*. phdthesis. Sorbonne Université; 2018. Accessed October 2, 2023. https://theses.hal.science/tel-02862784

51. Ferris FL, Wilkinson CP, Bird A, et al. Clinical Classification of Age-related Macular Degeneration. *Ophthalmology*. 2013;120(4):844-851. doi:10.1016/j.ophtha.2012.10.036

52. Marandi RZ, Gazerani P. Aging and eye tracking: in the quest for objective biomarkers. *Future Neurology*. 2019;14(4):FNL33. doi:10.2217/fnl-2019-0012

53. Shaikh AG, Otero-Millan J, Kumar P, Ghasia FF. Abnormal Fixational Eye Movements in Amblyopia. Martinez-Conde S, ed. *PLoS ONE*. 2016;11(3):e0149953. doi:10.1371/journal.pone.0149953

54. Ghasia F, Wang J. Amblyopia and fixation eye movements. *Journal of the Neurological Sciences*. 2022;441:120373. doi:10.1016/j.jns.2022.120373

55. Egaña J, Devia C, Mayol R, et al. Small Saccades and Image Complexity during Free Viewing of Natural Images in Schizophrenia. *Frontiers in Psychiatry*. 2013;4. Accessed October 2, 2023. https://www.frontiersin.org/articles/10.3389/fpsyt.2013.00037

56. Kaski D, Bronstein AM. Ocular Tremor in Parkinson's Disease: Discussion, Debate, and Controversy. *Frontiers in Neurology*. 2017;8. Accessed May 24, 2022. https://www.frontiersin.org/article/10.3389/fneur.2017.00134

57. Alexander RG, Macknik SL, Martinez-Conde S. Microsaccade Characteristics in Neurological and Ophthalmic Disease. *Frontiers in Neurology*. 2018;9. Accessed July 18, 2023. https://www.frontiersin.org/articles/10.3389/fneur.2018.00144

58. Sheehy CK, Bensinger ES, Romeo A, et al. Fixational microsaccades: A quantitative and objective measure of disability in multiple sclerosis. *Mult Scler*. 2020;26(3):343-353. doi:10.1177/1352458519894712

59. Poletti M. An eye for detail: Eye movements and attention at the foveal scale. *Vision Research*. 2023;211:108277. doi:10.1016/j.visres.2023.108277

60. Steinman RM, Cunitz RJ, Timberlake GT, Herman M. Voluntary Control of Microsaccades during Maintained Monocular Fixation. *Science*. 1967;155(3769):1577-1579. doi:10.1126/science.155.3769.1577

61. Collewijn H, Kowler E. The significance of microsaccades for vision and oculomotor control. *Journal of Vision*. 2008;8(14):20. doi:10.1167/8.14.20

62. Martinez-Conde S, Otero-Millan J, Macknik SL. The impact of microsaccades on vision: towards a unified theory of saccadic function. *Nat Rev Neurosci*. 2013;14(2):83-96. doi:10.1038/nrn3405